JOURNAL OF MATERIALS SCIENCE 4 (1969) 989–996

The Sintering of Activated CaO

W. L. DE KEYSER, R. WOLLAST, P. H. DUVIGNEAUD
Laboratory of Industrial Chemistry, University of Brussels, Brussels 5, Belgium

Received 1 May 1969

The sintering of CaO has been investigated from oxides of different "activity" resulting from the decomposition of $CaCO_3$ at 1000°C or $Ca(OH)_2$ between 600 and 1000°C.

Nitrogen adsorption, X-ray broadening and electrical conductivity were carried out in order to correlate the activity and the sintering ability.

Coble's models of first and intermediate stages of sintering can be applied to these oxides, considering that the self-diffusion coefficient of rate-controlling species (i.e. $D_{Ca^{2+}}$) is time dependent. The variations of $D_{Ca^{2+}}$ are connected with the presence of non-stoichiometric defects, related to the conditions of preparation, which are eliminated during sintering. The occurrence of such an excess of defects as well as the decrease of grain radius explain the improved sintering of the oxide activated by transformation of original carbonate to the hydroxide form.

1. Introduction

In an article published some years ago [1] one of us pointed out that the chemical activity of CaO obtained by dehydration of $Ca(OH)_2$ at 450° C is much greater than that of CaO resulting from the decomposition of $CaCO_3$ at 1000° C. This increased activity was linked with the considerable contraction that $Ca(OH)_2$ undergoes between 600 and 1000° C. It thus seemed reasonable that the CaO produced at low temperatures should be better suited to sintering.

This article is a very condensed account of investigations carried out over several years with the purpose of comparing the sintering behaviours of the oxide obtained by decomposition of $CaCO_3$ and by dehydration of $Ca(OH)_2$.

2. Materials and Experimental Methods

2.1. Shrinkage, Micrography

The CaO arising directly from the decomposition of $CaCO_3$ (designated below by C_C) is obtained by calcining a precipitated calcium carbonate (UCB) at 1000° C for 1 h.

The analysis of the oxide, carried out by emission spectroscopy and by atomic absorption gives the following wt %: Na = 0.03, Mg = 0.01, Al < 0.0004, Fe < 0.0005, Ba + Sr < 0.003. The CaO arising from the decomposition of $Ca(OH)_2$ (designated below by C_H) is prepared by dehydrating the hydroxide formed by hydrating C_C. The dehydration was carried out for 1 h at 600 and 1000° C.

The chemical analysis of this oxide gives the same impurity content as the preceding example. These two oxides are therefore chemically identical.

The calcium oxides thus prepared were compressed at 1500 kg/cm² into cylinders of 6 mm in diameter and 6 mm long, which were then sintered in air at various temperatures between 1100 and 1500° C.

The main physical properties of powders after calcination between 600 and 1000° C (surface area, pore distribution, grain and crystallite size) were investigated first. The adsorption isotherms for nitrogen were measured with a Perkin-Elmer sorptometer and interpreted using the BET theory which enabled us to calculate the specific surface area of the sample. The mean diameter of the particles was calculated assuming that CaO is made up of uniform spheres with no appreciable internal porosity.

We have, furthermore, carried out a detailed investigation of adsorption isotherms for CaO in order to determine whether or not the grains are porous, and by means of a method developed from the BJH [3], we have calculated not only the external surface of the solid but also the

surface of the pores. The X-ray technique was used to measure the crystallite size and the stresses in the samples. These experiments were carried out with a Philips recording diffractometer. Half-maximum widths of Kα peaks were computed by Rachinger's method [2]. In order to determine the dimensions of crystallites, we have distinguished the broadening (β) due to the size of the crystallites (βt) from that produced by internal deformations ($\beta\epsilon$) using Rachinger's equation.

Particle sizes were also directly measured on electron micrographs taken with an RCA electron microscope. Residual water was calculated by a radioactive method. CaO was tritiated and after calcination, residual H^3 was counted with a coincidence scintillation counter IDL 2032-2022: CaO was therefore dissolved in HCl and diluted in an organic scintillating medium (BBOT). We found that the limit of detection of water by this method is 0.1 ppm.

Sintering was followed by use of a Leitz dilatometer either at constant heating rate (160° C/h) or under isothermal conditions. We also measured the green and final densities by immersion in mercury using a modified analytical balance. Neck growth was observed on metallised polished sections with the aid of a JEOL JX A3A microprobe.

In connection with the dilatometric measurements of sintering, we followed the evolution of the electrical resistivity of the samples in the same range of temperature. These measurements were carried out at atmospheric pressure, under controlled atmosphere or vacuum. The electrical resistance of the samples placed between two platinum electrodes was determined with an alternative bridge operating at 1000 cylces/sec under 3.5 V.

3. Results

The difference in sintering ability of C_C and C_H is seen immediately from table I which enables one to compare the initial bulk densities with those obtained immediately after heat-treatment.

Although the initial density of C_H is considerably less than that of C_C, one obtains final bulk densities which are much higher for C_H than for C_C. It should be noted also that the dehydration temperature of C_H does not play a deciding role, since the densities after heating of the C_H samples prepared by dehydration at 600 and 1000° C are practically identical. The greater sintering ability of C_H thus seems to be determined chiefly by the nature of the starting product (C_H or C_C).

TABLE I Bulk densities of C_C and C_H obtained after heating for 22 h at the temperatures indicated.

Nature of the oxide	C_C	C_H	C_H
Preparation temperature	1000° C	600° C	1000° C
Initial bulk density	1.87	1.35	1.54
Sintering temperature	Final bulk density		
1100° C	1.92	2.17	2.11
1200° C	1.96	2.38	2.33
1300° C	2.00	2.60	2.62
1400° C	2.06	2.83	2.79

The dilatometric curves shown in fig. 1 confirm the differences in thermal behaviour of the two oxides. They also show that C_H undergoes a first shrinkage from 600 to 1000° C during which the density of the oxide increases from 1.35 to 1.65 g/cm³. The main shrinkage begins however in both cases at the same temperature, that is around 1100° C, which corresponds approximately to Tamman's temperature for CaO.

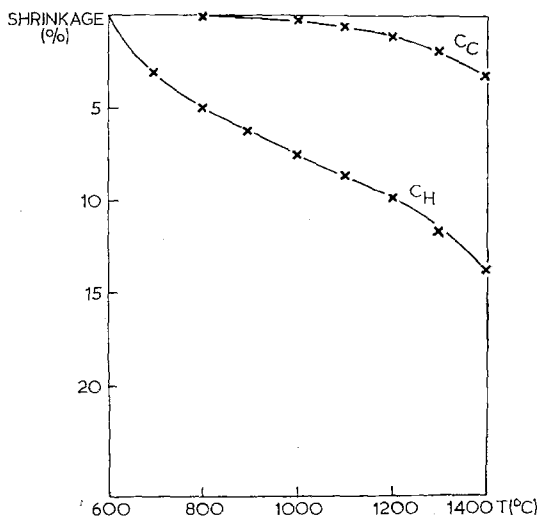

Figure 1 Dilatometric curves of C_C and C_H at a heating rate of 160° C/h.

An examination of the isothermal dilatometric curves (fig. 2) obtained above 1100° C also shows clearly the difference in activity of the two types of oxide at high temperature.

A comparative examination of micrographs of polished sections enables one to determine immediately the degree of sintering attained by each oxide in the time and temperature range considered. Figs. 3a and b are electron-micro-

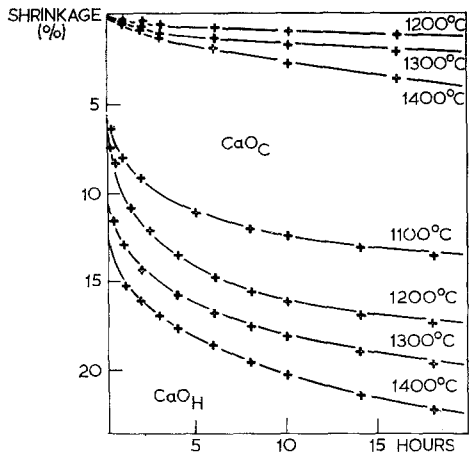

Figure 2 Isothermal dilatometric curves of C_C and C_H.

probe pictures obtained from back-diffused electrons. They show the morphology of C_H and C_C samples after sintering. In the case of C_C, the grains, which have maintained their original size, appear to be joined to each other by necks. This form is characteristic of the first sintering stage. The electron micrographs of C_H show a much greater degree of sintering during which the completely joined grains have very much increased in size. The pores are closed and dispersed in the bulk. This appearance corresponds to what is generally considered to be the intermediate stage of sintering.

3.1. Activity

It is known that one can activate a powder not only by increasing its intrinsic surface, but also by creating lattice defects, which facilitate the transport of matter by accelerating the diffusion rate of the determining element. Even though the importance of this method of preparation of a powder to determine its sintering ability has been demonstrated many times, the origin of the activation of the solid is generally less clear.

The comparative examinations of the activity of C_H and C_C deal with samples of C_H prepared by thermal treatment of the hydroxyde at 600 or 1000° C and of C_C obtained by heating the carbonate at 1000° C.

3.1.1. Dimensions of Solid Grains

We measured the size of CaO grains by utilising the adsorption isotherm and electron microscopy which enable one to calculate or measure the mean size of solid particles, and the broadening of X-ray diffraction lines which enables one to calculate the size of the crystallites. The results thus obtained are given in column 3 of table II. In column 2 can be found the mean dimensions obtained from direct measurements of particle size on electron micrographs. It can be seen that the agreement between the two methods of measurement is fairly good. The last column indicates the dimensions of crystallites obtained by analysing the broadening of the X-ray diffraction lines of lime.

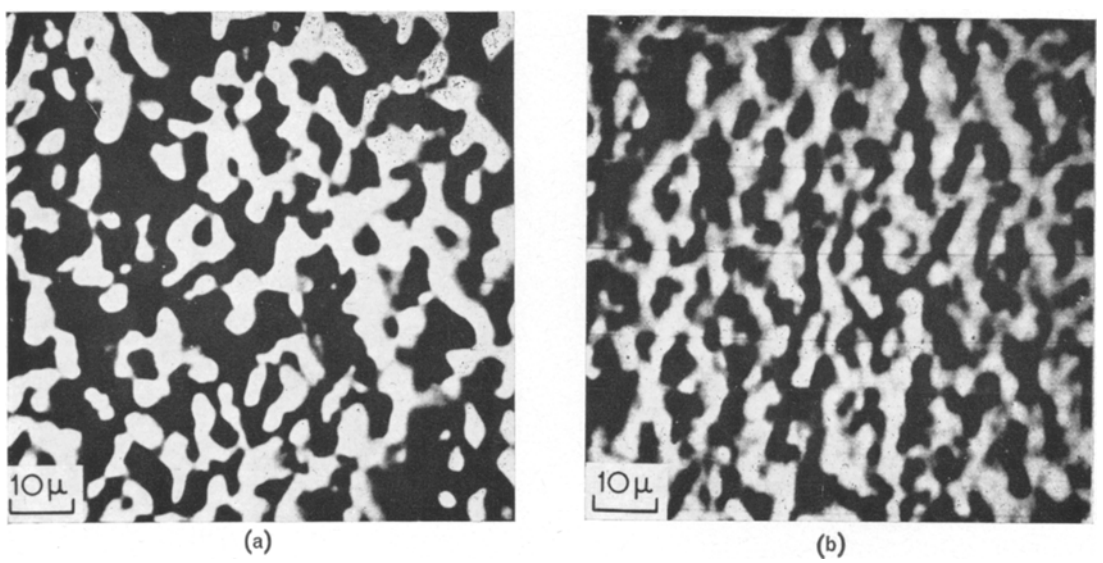

Figure 3 Back-scattered electrons image of (a) C_C, 1300° C, 20 h, (b) C_H, 1300° C, 20 h.

TABLE II Comparison of the dimensions of C_C and C_H by electron microscopy, from the adsorption isotherm, and by X-ray diffraction.

Sample	Electron microscope	Particle diameter (μm) BET	RX
C_H600	<0.2	0.065	0.047
C_H700	0.2	0.093	0.053
C_H800	0.25	0.176	0.048
C_H900	0.3	0.35	0.055
C_H1000	0.4	0.45	0.059
C_C1000	2.0	2.7	0.105

It can be seen that the crystallite diameter is always appreciably lower than the grain diameter measured by the BET method or by microscopy, with the exception of C_H 600 for which the three measurements are nearly in agreement.

The thermal evolution of C_H from 600 to 1000° C is shown only by an increase in the degree of agglomeration of the crystallites which join together to form grains attaining about 0.5μm at 1000° C.

It should be noted that the C_C grains are made up of crystallites having a diameter about twice as great as that of C_H crystallites. The diameter of grains produced at 1000° C is about 5 times greater for C_C than for C_H.

3.1.2. Deformations of the Crystal Lattice

A study of the broadening of X-ray diffraction lines has also demonstrated the existence of deformations in the C_H lattice. They disappear gradually when the sintering temperature passes from 600 to 1000° C. Their presence suggests the possibility of a significant ionic migration at low temperatures. However the lattice deformations of C_H do not enable one to explain the better sintering behaviour of this substance above 1000° C, since they do not persist above this temperature.

3.1.3. Porosity of CaO Grains

The results of these calculations indicate that only C_H 600 contains an appreciable porosity and show that its external surface area is 16.2 m^2/g and the area of the pores is 7.3 m^2/g. The resulting porosity is 6.24% and the mean diameter of the pores lies around 70 Å. The disappearance of this porosity between 600 and 1000° C must correspond to an increase of 6%. This result partly explains the shrinkage curve observed below 1000° C in fig. 1.

3.1.4. Presence of Residual Water in C_H

It might be supposed that the increased activity of C_H is due to the presence in the CaO lattice of residual OH groups which may persist at high temperatures. In order to check this hypothesis we measured the quantity of tritium present in samples of tritiated lime after dehydration at 600 and 1000° C.

In spite of the fact that a very sensitive method was used, the presence of OH groups could not be detected, except in the case of C_H obtained by heating at 600° C, for which the amount of residual water was 6×10^{-7} g H_2O/g CaO. The activation of C_H cannot therefore be explained by the presence of residual OH in the lattice.

3.1.5. Electrical Conductivity

We finally studied in detail the electrical properties of the various samples of CaO. The electrical conductivity enables one to determine directly the number and type of defects present in a crystal lattice; its importance in studying suitability for sintering is therefore evident.

We confirmed that the conductivity of a monocrystal of CaO is purely electronic in the temperature range of interest, but the charge-carriers in it are closely related to the presence of cationic defects. The thermal defects present may be described by the following equilibrium:

$$\tfrac{1}{2}O_{2(gas)} \rightleftharpoons V_{Ca}^{2+} + O^{2-} + 2\oplus$$

Polycrystalline samples of C_C and C_H sintered at high temperatures show conductivities equal to those of the monocrystal, which rules out the existence of a large conductivity at grain-boundaries.

On the other hand, CaO samples arising from decarbonation or dehydration have an excess electrical conductivity which decreases on heat-treatment above 1100° C, falling to the equilibrium value obtained for the monocrystal. Fig. 4 shows the variation in electrical conductivity of pellets of the same type as those used for dilatometric tests.

In the graphical representation which we have adopted, the ordinate is σ_t/σ_e, where σ_e represents the conductivity toward which the sample tends at each temperature after a long period of heating. As the conductivity is proportional to n, the number of vacancies, one has:

$$\sigma_t/\sigma_e = n_t/n_e .$$

4. Interpretation of the Results

4.1. Elimination of Excess Vacancies

The preparation of CaO from $Ca(OH)_2$ or

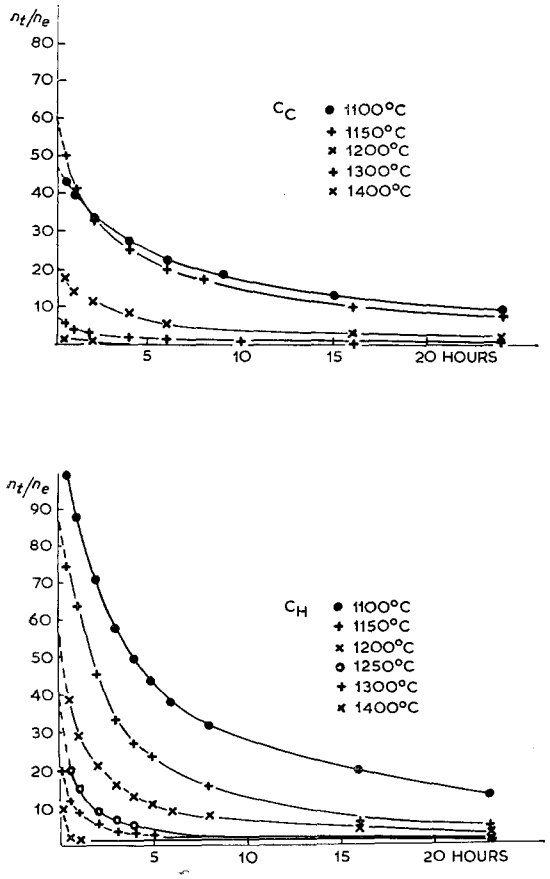

Figure 4 Comparison of the calculated curves for the elimination of excess vacancies from Serin and Ellickson's equation and the experimental results.

$CaCO_3$ introduces into the lime lattice a certain number of excess vacancies which disappear at an appreciable rate above 1100° C.

We have been able to show that the evolution of the vacancies can be very exactly interpreted by a mechanism involving diffusion of an initial excess n_0 of vacancies, uniformly distributed in the bulk of the solid. Such a mechanism obeys Serin and Ellickson's equation [4]:

$$1 - \frac{n_0 - n_t}{n_0 - n_e} = \frac{6}{\pi^2} \sum_n \frac{1}{\pi^2} \exp \frac{-n^2 \pi^2 D_m t}{r^2} \qquad (1)$$

Using this relation and knowing n_0 and n_e, we were able to calculate the n_t/n_e curves. Referring to fig. 4, it can be seen that the experimental points lie on the curves calculated in this way. This verifies the hypothesis which we put forward above concerning the uniform distribution of excess vacancies and their diffusion mechanism.

Using these curves, we have thus been able to calculate the variation of D_m (diffusion coefficient for the vacancies) with temperature, and hence the heat of activation. The value found (30 kcal/mole) is close to that determined by Gupta (34 kcal/mole) [5]. The elimination mechanism is the same for C_H as for C_C. The only difference is the initial number of vacancies, which is twice as great for C_H as for C_C.

4.2. Sintering Mechanism in the Presence of an Excess of Vacancies

We shall consider in turn the first two stages of sintering, taking into account the fact that the excess of vacancies present in CaO involves an increase in the self-diffusion coefficient and supposing that the distribution of vacancies does not otherwise influence the phenomenon.

4.2.1. First Stage of Sintering

Without Excess Vacancies: As we have seen above (fig. 3) the sintering of C_C does not go further than the first stage. At 1500° C, the number of excess vacancies is negligible. At this temperature, the contraction of C_C obeys a law of the form

$$y = kt^{0.45} \qquad (2)$$

which indicates that the first stage obeys Coble's equation [6]:

$$\frac{dy}{dt} = \left[\frac{2\, a^3 \gamma D_a}{kTr^3}\right]^{1/2} t^{-1/2}, \qquad (3)$$

where D_a = self-diffusion coefficient.

Influence of Uniformly Distributed Excess Vacancies: Coble's equation can be applied directly only if D_a is constant, but this is not the case here. D_a becomes then an apparent coefficient which varies with the number of vacancies:

$$D_a = ND_m = N\,A \exp\left[-\frac{E_m}{RT}\right], \qquad (4)$$

E_m = energy of activation for vacancy diffusion, N = fraction of vacancies related to total number of sites, D_m = diffusion coefficient for the vacancies.

When the vacancies are controlled solely by thermal agitation:

$$n_e = k \exp\left(-\frac{E_f}{RT}\right). \qquad (5)$$

The self-diffusion coefficient can then be written

$$D_{a,e} = k\,A \exp\left[-\frac{E_f + E_m}{RT}\right] = k\,A \exp\left(-\frac{E_D}{RT}\right), \quad (6)$$

E_f = energy of formation of the vacancies,
E_D = energy of activation for self-diffusion.

If the number of vacancies is controlled by a process other than thermal agitation, such as the presence of impurities or the method of preparation, one has, at time t,

$$D_a = \frac{n_t}{n_e} D_{a,e}. \quad (7)$$

In order to use equation 3 in which D_a varies according to 7, a relation which gives n_t as a function of time must be introduced. This can be done as we have shown by Serin and Ellickson's equation. This series converges quickly and the first term above can be used for sufficiently long times.

The variation of the number of excess vacancies can then be written in the form

$$\frac{n_t}{n_e} = 1 + a\left[\frac{n_0}{n_e} - 1\right] \exp(-bt). \quad (8)$$

Substituting this relation into Coble's equation one finally obtains

$$\frac{dy}{dt} = \left[\frac{\gamma a^3 D_{a,e}}{kT r^3}\right]^{1/2} \left[\frac{1 + a\left(\frac{n_0}{n_e} - 1\right)\exp(-bt)}{t}\right]^{1/2}. \quad (9)$$

This equation has been integrated using an analog computer. For short times, the variation of n_t/n_e was calculated using tabulated values of Serin and Ellickson's equation, which were then introduced into the machine in the form of initial conditions.

We have thus calculated the sintering curves of C_C at 1300, 1350 and 1400° C, taking into account the initial number of vacancies and their rate of elimination, determined experimentally by electrical conductivity measurements.

The results are represented as a logarithmic function in fig. 5a which also enables one to compare the calculated curves with the experimental data. It follows moreover that the activation energy of $D_{a,e}$ is 85 kcal/mole.

The presence of these vacancies also enables one to explain why the first stage of the sintering of C_H takes place at a considerably lower

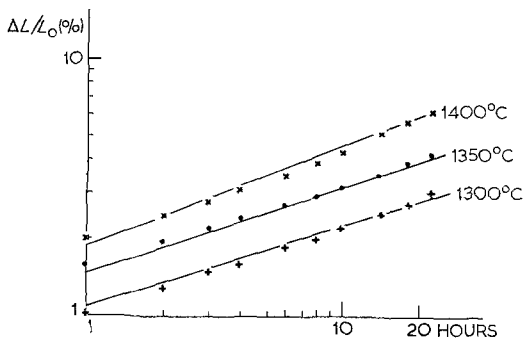

(a)

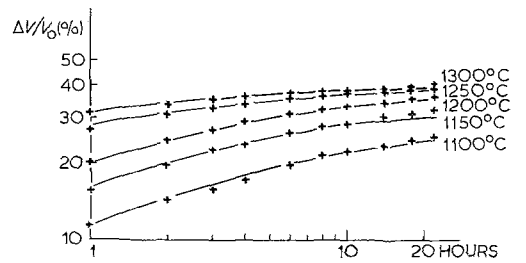

(b)

Figure 5 (a) Comparison of the calculated curves for the sintering of C_C from equation 10 and the experimental results. (b) Comparison of the calculated curves for the sintering of C_H from equation 14 and the experimental results.

temperature than C_C. If one does not take into account the excess of vacancies, Coble's equation shows that the initial sintering rates of C_C and C_H will be equal when

$$\left[\frac{D_a}{r^3 T}\right]_{C_C} = \left[\frac{D_a}{r^3 T}\right]_{C_H},$$

that is

$$\left[\frac{\exp\left(-\frac{E_D}{RT}\right)}{r^3 T}\right]_{C_C} = \left[\frac{\exp\left(-\frac{E_D}{RT}\right)}{r^3 T}\right]_{C_H}. \quad (10)$$

Taking into account only the grain radii of C_H and C_C, it is found that the sintering rate of C_H should be equal to that of C_C at 1400° C at a temperature of 870° C. Now the experimental results show that at this temperature, the first stage of sintering of C_H is practically complete (see fig. 1).

On the other hand, if one takes into account not only the different radii but also the excess of

vacancies, the initial rates are given by

$$\left[\frac{n_0 D_m}{r^3 T}\right]_{C_C} = \left[\frac{n_0 D_m}{r^3 T}\right]_{C_H},$$

that is

$$\left[\frac{n_0 \exp\left(-\frac{E_m}{RT}\right)}{r^3 T}\right]_{C_C} = \left[\frac{n_0 \exp\left(-\frac{E_m}{RT}\right)}{r^3 T}\right]_{C_H}. \quad (11)$$

It is then found that at 500° C, the rate of sintering of C_H is equal to that of C_C at 1400° C. This is in qualitative agreement with what one observes experimentally since the sintering of C_H begins immediately after the phenomenon of dehydration.

4.2.2. Second Stage of Sintering

The excess holes modify the kinetics of the second stage of sintering in a similar way to the previous case. Coble's relation, which describes the intermediate stage of sintering

$$\frac{dP}{dt} = \frac{d\triangle V}{V} = \frac{35\pi\gamma a^3_0 D_{a(t)}}{G^3(t)}, \quad (12) \text{ cf. } [8, 9]$$

also contains the self-diffusion coefficient $D_a(t)$, which varies as previously with the excess of defects.

An additional difficulty in the integration of this equation arises from the factor G, the diameter of the tetrakaidecahedral grain, which increases with time. From the experimental observations of Coble, Clare and Gupta [8–11], Coble put $G(t) = At^u$, where $u = 1/3$.

From measurements carried out on optical and electron micrographs, we have been able to determine the grain growth equation between 1100 and 1400° and hence obtain $G(t)$. For times less than 20 h, we found:

at 1100, 1150 and 1200° C : $G = A_{(T)}\, t^{0.18}$
at 1250° C : $G = B_{(T)}\, t^{0.22}$
at 1300° C : $G = C_{(T)}\, t^{0.28}$

Above 1300° C $G(t)$ tends to an exponent of t equal to 1/3, which is generally observed for dense compacts in which porosity is closed; this is not the case in the range of densification considered. In our case therefore, we cannot introduce the exponent 1/3 into equation 12.

Integration of Coble's equation has been carried out for small ranges of $\triangle V/V$ such that the values of n_t/n_e may be considered constant. In the general case one has:

$$\int_{V_1}^{V_2} d\frac{\triangle V}{V_0} = \frac{35\pi\gamma a_0^3}{A_{(T)}} \left[\frac{n_t}{n_e}\right]_{t_1}^{t_2} D_{a,e} \int_{t_1}^{t_2} \frac{dt}{(t^u)^3},$$

where u varies between 0.18 and 0.28.

The variations of $\triangle V/V$ calculated in this way have been compared with the corresponding experimental variations given in fig. 5b. The agreement is very satisfactory. The activation energy for diffusion calculated from equation 13 is equal to 85kcal. This is in perfect agreement with that obtained for the initial stage of sintering.

The values of the diffusion coefficients deduced from the sintering experiments have been compared with literature, values resulting from self-diffusion measurements [5, 7] (fig. 6).

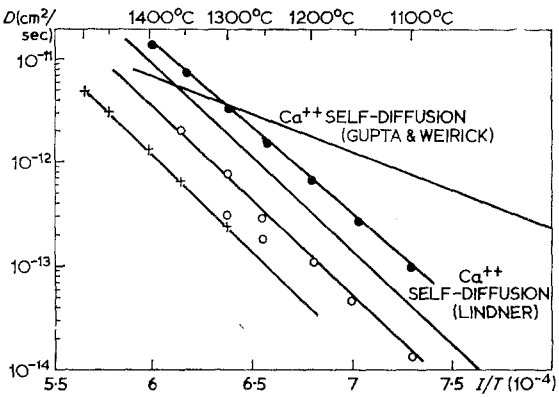

Figure 6 Comparison of diffusion coefficients in CaO from diffusion and sintering measurements. + our values: first stage of sintering C_C. ○ our values: intermediate stage of sintering C_H. ● our values: electrical conductivity of sintered C_C and C_H taking into account transport number values of Ca^{2+} from Lindner's experiments.

The coefficients $D_{a,e}$ for the initial and intermediate stages of sintering are of the same order of magnitude as Lindner's values of $D_{Ca^{2+}}$ [7]. The activation energies of these two stages (85 kcal/mole) correspond to the activation energy for self-diffusion of Ca^{2+} (81 kcal). In our case diffusion is therefore intrinsic above 1100° C. On the other hand, the activation energy measured by Gupta and Weirick [5] (30 kcal) corresponds to the migration of Ca^{2+}. It seems that in their experiments the holes are not of thermal origin, but arise from the presence of impurities of excess defects resulting from quenching.

The agreement between $D_{a,e}$ and $D_{Ca^{2+}}$ seems to indicate that Ca^{2+} is the rate-controlling species in CaO diffusion and this would be

consistent with the large ionic radius of Ca^{2+} (0.99 Å).

The case of CaO seems therefore to be analogous to that of $Zr_{1-x}Ca_xO_2$ and UO_{2+x} pointed out by Rhodes and Carter [12], whose ionic radii are comparable with those of Ca^{2+} (Zr^{4+} : 0.79 Å; U^{4+} : 0.97 Å).

5. Conclusions

The preparation of CaO from $Ca(OH)_2$ or $CaCO_3$ introduces into the lime lattice a large number of excess vacancies which are eliminated above 1100° C. Moreover the C_H grains are initially about 50 times smaller than the C_C grains.

The presence of these excess vacancies appreciably increases the rate of matter transport and greatly reduces the activation energy of the phenomenon, thus considerably favouring sintering.

As a consequence of the extremely small size of the particles and of the presence of uniformly distributed excess vacancies, the first stage of the sintering of C_H occurs immediately after the dehydration of the $Ca(OH)_2$.

For C_C which is made up of larger grains and contains fewer vacancies, appreciable sintering is not observed to begin below 1300°.

The second stage of sintering of C_H takes place at 1100° C and above, that is in a range of temperature in which the excess vacancies are still numerous and can play a favourable role in densification.

References

1. W. L. DE KEYSER, *Bull. Soc. Chim. Belg.* **60** (1951) 516.
2. W. A. WOOD and W. A. RACHINGER, *J. Inst. Met.* **75** (1948) 571.
3. E. P. BARRET, L. G. JOYNER, and P. P. HALENDA, *J. Amer. Chem. Soc.* **73** (1951) 373.
4. B. SERIN and R. T. ELICKSON, *J. Chem. Phys.* **9** (1941) 742.
5. Y. P. GUPTA and L. J. WEIRICK *J. Phys. Chem. Solids* **28** (1967) 811.
6. R. L. COBLE, *J. Amer. Ceram. Soc.* **41** (1958) 55.
7. R. LINDNER, *Scand. Chem. Acta* **6** (1952) 468.
8. R. L. COBLE, *J. Appl. Phys.* **32** (1961) 93, 787.
9. T. E. CLARE, *J. Amer. Ceram. Soc.* **49** (1966) 159.
10. R. L. COBLE, Proceedings sec. Conf. on Sintering phenomena, edited by Kuczynski (1965) p. 423.
11. Y. P. GUPTA and R. L. COBLE, *J. Amer. Ceram. Soc.* **51** (9) (1968) 512.
12. W. H. RHODES and R. E. CARTER, *J. Amer. Ceram. Soc.* **49** (5) (1966) 244, 268.